Industrielle Gemeinschaftsforschung

Schlussbericht

zu IGF-Vorhaben Nr. 177 EN

Thema

Grundlegende experimentelle und numerische Untersuchungen zur Ablagerungsbildung und -zersetzung aus AdBlue in SCR-Systemen

Berichtszeitraum

01.01.2017 - 30.04.2019

Forschungsvereinigung

Forschungsvereinigung Verbrennungskraftmaschinen e. V.

Forschungseinrichtung(en)

Institut für Technische Chemie und Polymerchemie (ITCP)
Karlsruher Institut für Technologie

Institut für Fahrzeugantriebe und Automobiltechnik (IFA)
Technische Universität Wien (TUW)

Karlsruhe, Wien, 01.09.2019	Prof. Olaf Deutschmann, Prof. Bernhard Geringer
Ort, Datum	Name und Unterschrift aller Projektleiterinnen und Projektleiter der Forschungseinrichtung(en)

Gefördert durch:

Bundesministerium für Wirtschaft und Energie

aufgrund eines Beschlusses des Deutschen Bundestages

Forschungsnetzwerk Mittelstand

AdBlue Deposits

Project no. 1262

Abschlussbericht | Final report EN (AB)

---

1 | Institut für Technische Chemie und Polymerchemie | Institute of Technical Chemistry and Polymer Chemistry **(ITCP)**
Prof. Dr. Olaf Deutschmann | Karlsruher Institut für Technologie (KIT)

2 | Institut für Fahrzeugantriebe und Automobiltechnik | Institute for Powertrains and Automotive Technology **(IFA)**
Prof. Dr. Bernhard Geringer | Technische Universität Wien (TUW)

Thema | Full title:	Grundlegende experimentelle und numerische Untersuchungen zur Ablagerungsbildung und -zersetzung aus AdBlue in SCR-Systemen | Fundamental experimental and numerical investigation on the deposit formation and decomposition from AdBlue in SCR systems
Laufzeit | Duration:	01.01.2017 – 30.04.2019
Fördergeber | Funding:	Bundesministerium für Wirtschaft und Energie / Arbeitsgemeinschaft industrieller Forschungsvereinigungen / Collective Research Networking | Federal Ministry for Economic Affairs and Energy / Industrial Collective Research / Collective Research Networking (BMWi/AiF) Bundesministerium für Verkehr, Innovation und Technologie | Austrian Ministry for Transport, Innovation and Technology (BMVIT) Österreichische Forschungsförderungsgesellschaft | Austrian Research Promotion Agency (FFG) Forschungsvereinigung Verbrennunskraftmaschinen e. V. | Research Association for Combustion Engines eV (FVV)
Fördernr. | Funding no:	177 EN, 601262
Obmann | Chairperson:	Johannes Scholz (IAV)
Bearbeiter | Coordinators:	Dr. Marion Börnhorst (ITCP) Christian Kuntz (ITCP) Uladzimir Budziankou (IFA) Prof. Dr. Thomas Lauer (IFA)

Gefördert durch:
Bundesministerium für Wirtschaft und Energie
aufgrund eines Beschlusses des Deutschen Bundestages
Forschungsnetzwerk Mittelstand
Industrielle Gemeinschaftsforschung
FVV Forschungsvereinigung Verbrennungskraftmaschinen

Danksagung

Dieser Bericht ist das wissenschaftliche Ergebnis einer Forschungsaufgabe, die von der Forschungsvereinigung Verbrennungskraftmaschinen (FVV) e.V gestellt und am Institut für Technische Chemie und Polymerchemie des Karlsruher Institut für Technologie unter Leitung von Prof. Dr. Olaf Deutschmann und Prof. Dr. Jan-Dierck Grunwaldt und am Institut für Fahrzeugantriebe und Automobiltechnik der Technischen Universität Wien unter Leitung von Prof. Dr. Bernhard Geringer bearbeitet wurde.

Die FVV dankt den Professoren Prof. Dr. Olaf Deutschmann und Prof. Dr. Bernhard Geringer und den wissenschaftlichen Mitarbeitern Dr. Marion Börnhorst (ITCP), Christian Kuntz (ITCP), Uladzimir Budziankou (IFA) und Prof. Dr. Thomas Lauer (IFA) für die Durchführung des Vorhabens. Das Vorhaben wurde von einem Arbeitskreis der FVV unter der Leitung von Johannes Scholz (IAV) begleitet. Diesem projektübergreifenden Ausschuss gebührt unser Dank für die große Unterstützung.

Das IGF-Vorhaben Nr. 177 EN der Forschungsvereinigung Verbrennungskraftmaschinen (FVV) e.V wurde über die AiF im Rahmen des Programmes zur Förderung der Inustirelle Gemeinschaftsforschung und –entwicklung (IGF) vom Bundesministerium für Wirtschaft und Energie (BMWi) aufgrund eines Beschlusses des Deutschen Bundestages gefördert. Der Anteil der TU Wien wurde vom Bundesministerium für Verkehr, Innovation und Technologie (BMVIT) über die Österreichische Forschungsförderungsgesellschaft (FFG) gefördert.

Acknowledgement

This report is the scientific result of a research project undertaken by the FVV (The Research Association for Combustion Engines eV) and performed by the Institute for Chemical Technology and Polymer Chemistry (ITCP) at Karlsruhe Institute of Technology (KIT) under the direction of Prof. Dr. Olaf Deutschmann and Prof. Dr. Jan-Dierck Grunwaldt and by the Institute of Powertrains and Automotive Technology (IFA) at TU Wien (TUW) under the Direction of Prof. Dr. Bernhard Geringer.

The FVV would like to thank the professors Deutschmann, Grunwaldt and Geringer and their scientific assistants – Dr. Marion Börnhorst (ITCP), Christian Kuntz (ITCP), Uladzimir Budziankou (IFA) and Prof. Dr. Thomas Lauer (IFA) – for the implementation of the project. Special thanks are due to the AiF (German Federation of Industrial Research Associations eV) for funding of the project within the framework of the collective research networking (CORNET) programme. The project was conducted by an expert group led by Johannes Scholz (IAF). We gratefully acknowledge the support received from the chairman and from all members of the project user committee.

The research was carried out in the framework of the industrial collective programme (IGF/CORNET no. 177 EN). It was supported by the Federal Ministry for Economic Affairs and Energy (BMWi) through the AiF (German Federation of Industrial Research Associations eV) based on a decision taken by the German Bundestag. The work of TU Wien was funded by the Federal Ministry of Transport, Innovation and Technology (BMVIT) through the Austria Research Promotion Agency (FFG).

Kurzfassung

Basierend auf immer strengeren Emissionsrichtlinien ist eine zukünftige weitere Minimierung der Stickoxid (NOx) Emissionen für Dieselmotoren notwendig. Die selektive katalytische Reduktion (SCR) ist dabei in Verbindung mit anderen Abgasnachbehandlungskomponenten eine effiziente und weit verbreitete Methode zur Reduzierung der Stickoxide. Bei SCR Anlagen wird Harnstoff in Form einer Harnstoff-Wasser-Lösung (UWS) in den Abgasstrang injiziert. Die Verdampfung des Sprays und thermische Zersetzung des Harnstoffs führen zur Ammoniakentwicklung vor dem SCR-Katalysator. Die Tropfen der Harnstoff-Wasser-Lösung prallen häufig auf die heiße Abgaswand, wo sie in niedrigen Lastpunkten Wandfilm bilden. Angesammelter Wandfilm wiederum kann zu starker Ablagerungsbildung durch Harnstoffkristallisation und Bildung von Nebenprodukten führen, die die Funktion des SCR Systems beeinträchtigen.

Diese Arbeit erforschte die Interaktion von AdBlue-Sprays mit heißen Abgaswänden, die resultierende Wandfilmbildung sowie das Entstehen fester Ablagerungen aus dem flüssigen Film. Für Untersuchungen im Anwendungsmaßstab wurden ein Laborgasprüfstand am KIT und ein Motorprüfstand an der TUW aufgebaut, die Experimente zur Film- und Ablagerungsbildung unter realitätsnahen Bedingungen ermöglichten. Die experimentell erzeugten, festen Ablagerungen wurden zur detaillierten Analyse der Topologie und der chemischen Zusammensetzung entnommen und durch thermogravimetrische Analyse (TGA) und Hochleistungsflüssigkeitschromatographie (HPLC) untersucht.

Basierend auf kinetischen Daten aus den Experimenten wurde ein bestehendes kinetisches Modell der Harnstoffzersetzung erweitert. Zusammen mit weiterentwickelten Modellen für die Spray/Wand-Interaktion, den Wärmeübergang und einem Ansatz zur deutlichen Beschleunigung der Simulationen, wurden erstmals sowohl physikalische als auch chemische Prozesse in der Mischstrecke von SCR Systemen in 3D-CFD-Simulationen abgebildet. Weiterhin wurde ein neues, kinetisches Modell vorgestellt, welches hauptsächlich auf thermodynamischen Daten und Gleichgewichtsprozessen basiert und eine detaillierte Vorhersage der Zersetzung von Harnstoff und Nebenprodukten und den experimentell auftretenden Effekten ermöglicht.

Das Ziel des Forschungsvorhabens ist erreicht worden.

Abstract

Based on legislation for diesel engines a further minimization of emissions of nitrogen oxides (NOx) is essential. The selective catalytic reduction (SCR) is therefore an efficient and widely used method to reduce nitric oxide emissions, frequently in combination with other emission control devices. In SCR systems, urea is injected into the tailpipe as a urea-water solution (UWS). Water evaporation and decomposition of the urea content produce gaseous ammonia upstream of the SCR catalyst. The droplets of the UWS frequently impinge on the hot surfaces of the exhaust line where they may form liquid film at part load operating points. Accumulated liquid film on the other hand can induce formation of solids due to urea crystallization and by-product formation, which impedes the SCR efficiency.

This work investigated the interaction of AdBlue sprays with hot tail pipe walls, the resulting wall film formation and the precipitation of solid deposits from liquid film. For investigations in application scale, a lab test bench at KIT and an engine test bench at TUW were installed, which enabled experiments on film and deposit formation under realistic conditions. Solid deposits that were generated during the experiments were sampled for detailed analysis of topology and chemical composition by thermogravimetrical analysis (TGA) and high performance liquid chromatography (HPLC).

Based on kinetic data from the experiments an existing kinetic model for urea decomposition was extended. Together with enhanced models of spray/wall interaction, heat transfer and an approach to substantially speed-up the simulations, for the first time physical as well as chemical processes in the mixing section of SCR systems were depicted in 3D-CFD simulations. Furthermore a new kinetic model was introduced that is mainly based on thermodynamic data and equilibrium processes and which allows a detailed prediction on urea decomposition and deposit formation with all upcoming experimental effects.

The objective of the research project was achieved.

1 Introduction

Exhaust gas after-treatment of diesel engines has remained a complex and challenging task during the past decades. Not only the continuously tightened emission regulations but also the need for higher fuel efficiency have raised a strong demand for efficient exhaust gas aftertreatment technologies.

The favored method to reduce nitrogen oxides is selective catalytic reduction (SCR) using ammonia as reducing agent. Due to security issues, passenger cars cannot be equipped with an ammonia tank. Consequently, ammonia is provided in form of a urea-water solution, which decomposes through thermolysis and hydrolysis after being dispersively dosed into the hot exhaust pipe. The droplets of the UWS frequently impinge on the hot surfaces of the exhaust line where they may form liquid film at part load operating points. Depending on temperature and residence time, urea crystallizes from the evaporating liquid films. Besides decomposition of urea to ammonia and CO_2, the highly reactive intermediate isocyanic acid is formed promoting urea side reactions. By-products like biuret, triuret, cyanuric acid or ammelide may evolve from the liquid film forming deposits, which are hard to remove from mixer elements and walls. Solid deposits strongly decrease system efficiency by impeding ammonia generation and uniformity. Further, they affect the surface properties of wall and mixer and thereby influence the flow field and further impingement.

Numerous experimental studies have focused on the experimental investigation of spray injection and mixing, droplet evaporation, impingement phenomena, wall films and deposit formation.

Numerical simulation of physical and chemical processes in the mixing section of SCR systems is a fundamental tool for system design and optimization. In particular, a correct prediction of ammonia generation and homogenization is important for dimensioning system geometry and catalyst size. Furthermore, simulation of harmful deposit formation is desired in order to be useful for aftertreatment engineering. CFD simulations are a powerful tool to study the complex physical interactions in the tailpipe. However, including chemical reactions in multiple phase simulations represents a challenge of high numerical effort. Especially the consideration of urea reactions in the liquid film in CFD simulations has remained a challenging task.

The project target is therefore to fundamentally understand and model the deposition process of solids in the tailpipe section downstream of the AdBlue injection point. In detail, the dependence of deposit formation from the operating conditions namely spray and exhaust properties, the injection position as well as the temperature of the turbulent exhaust flow are experimentally investigated. Furthermore, a comprehensive modeling approach with a kinetic model for urea decomposition is established to predict deposit formation in SCR systems.

2 Project Execution and Results

The following sections present the results of the different work packages of this project including experimental and numerical investigations on deposit formation from liquid urea. In Figure 2.1 the project schedule with all work packages and the three milestones is shown.

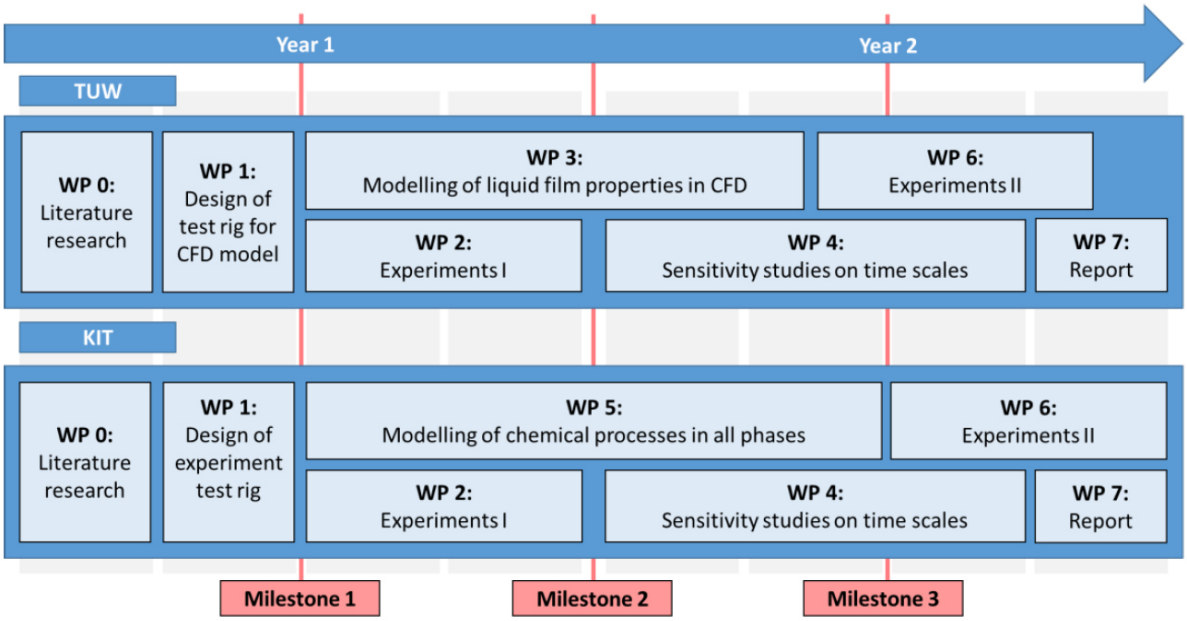

Figure 2.1: Project schedule stating the different working packages and milestone.

In WP 1 a lab test bench at KIT and an engine test bench at TUW with defined boundary conditions were designed and installed, which was the goal of milestone 1. The setups, analytical methods and experimental procedure are described in Section 2.1. First experiments with steady state conditions were conducted to investigate wall wetting, liquid pathways and deposit formation on both benches in WP 2. With analysis of the created deposits, milestone 2 was achieved. In WP 3, a CFD model was created at TUW to model injection, spray/wall interaction and impingement heat transfer. The CFD simulations were carried out with the CFD code StarCCM+ v13.06, which was agreed among all project members. Modeling of urea decomposition mechanism was carried out in a 0D multiphase tank reactor model with the DETCHEM software package, named DETCHEM^{MPTR}. Furthermore, an implementation into the CFD simulations was done during WP 5. When reaching milestone 3, the general capability to model deposit formation was demonstrated. The combined modeling approach was tested at different operating conditions and deposit formation on both test benches. A good agreement between simulated and experimentally observed deposits could be demonstrated. In WP 6, the second experimental part focused on transient conditions and possibilities to remove existing deposits. The report from WP 7 brought all parts together and documented the comprehensive and consistent work flow.

2.1 Experimental setups and procedure

In the following, setups and methods at KIT and TUW for experimental investigations on deposit formation and their characterization are presented. With designing and installation of the two test benches WP 1 and milestone 1 were completed.

2.1.1 Lab test bench at KIT

A hot gas lab test bench was set up to derive solid deposits from UWS injection under well-defined conditions over a wide range of operating parameters. A schematic illustration of the test rig is given in Figure 2.2.

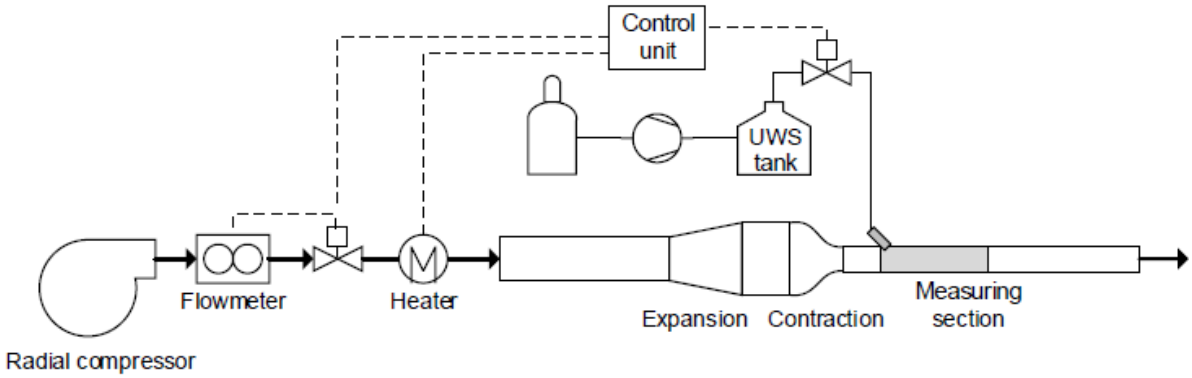

Figure 2.2: Schematic of hot gas lab test bench setup for deposit generation.

After the gas passes a radial compressor, a flowmeter, an electrical gas heater it flows into a expansion and smoothing section to eliminate swirls. Downstream of the smoothing section the flow channel is contracted to a rectangular cross section of 60 mm x 30 mm representing the cross-sectional area of the measurement section with a length of 200 mm. The measuring section provides optical access through borosilicate windows from three sides and a 1 mm steel bottom wall enables contact free temperature measurements infrared thermography. A commercial three -hole injector for UWS dosage, which features a droplet Sauter diameter of $d_{32} = 168\,\mu m$ and a static mass flow of 3.1 kg h^{-1}, is mounted into the measuring section by an injection angle of 33°. An outlet section connected to the exhaust system follows the measurement section downstream.

The setup provides a wide range of operating conditions for experiments, which are displayed in Table 2.1.

Table 2.1: Operating range of test rig for investigations on deposit formation.

Operating parameter	Symbol	Unit	min	max
Gas temperature	T_g	°C	25	350
Gas flow	$\dot{V}_g$	L min^{-1}	0	3200
Gas velocity	u_g	m s^{-1}	0	30
Reynolds number	Re	-	0	75000
UWS mass flow	$\dot{m}_{UWS}$	kg h^{-1}	0	5.5

2.1.2 Engine test bench at TUW

For investigations on spray impingement and deposit formation, a measuring section with optical access consisting of an AdBlue injector mount and a stainless steel X5CrNi18-10 target plate was designed in order to study deposit formation under engine typical operating conditions. The distance between the injector tip and the surface of the impingement plate was approximately 110 mm. Figure 2.3 shows the CAD-model and the final setup at the test bed. An inlet section with a small cone angle followed by an uncoated substrate was implemented in order to generate a uniform, unidirectional flow with fine-scale, isotropic turbulence. Downstream of the measuring section further uncoated substrate separated any liquid urea from the exhaust gas.

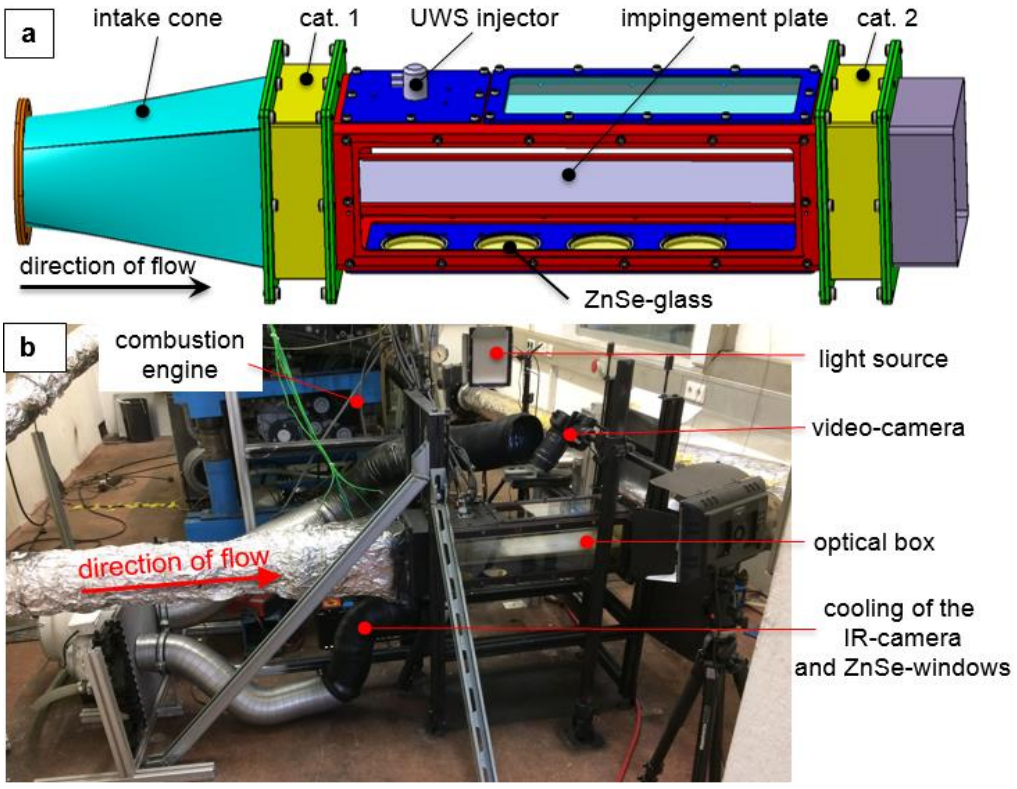

Figure 2.3: (a) CAD-model of the optical box, (b) set up of the engine test bench for investigations of deposit formation and decomposition.

A two-stage turbocharged heavy duty diesel engine with 10.5 liter displacement was used as exhaust gas supply. The engine was equipped with a DOC and DPF catalyst. Therefore, a clean exhaust gas with a desired mass flow of up to 1200 kg/h and a gas temperature of up to 500 °C could be supplied to the measuring section. For temperature measurements at the inlet, a thermocouple was placed in the center of the intake cone close to the surface of the first catalyst. The mass flow of the exhaust gas is measured with a mass flow meter of the type “Sensyflow FMT700-P”. The following measurement techniques were applied in order to characterize and document the AdBlue spray, the wallfilm and deposit formation:

Table 2.2: Applied measurement techniques

Parameter	Measurement technique	System	Access	Specification
spray	high-speed imaging	PCO.dimax HD	quartz glass	• framerate 3,000 Hz • exposure time 7 µs
wallfilm, deposits	video recording	Canon EOS 650D	quartz glass	• framerate of 24 Hz • resolution of 640x480 pixel • LED lights
droplet size	laser diffraction	SprayTec	quartz glass	• measuring duration 10 s • measuring volume with 10 mm diameter • 25,000 samples
material temperature, wallfilm	infrared thermography	thermoIMAGER TIM 640	ZnSe-windows	• temp. range -20 °C to 900 °C • framerate of 32 Hz • resolution of 640x480 pixel • black coating of the structure

Three AdBlue injectors are chosen for the experimental investigations with the goal to cover a wide range of Weber-numbers (We) and specific area loads of the sprays' footprint, which are known to have crucial impact on the spray impingement regimes and the wall cooling. The most important spray characteristics were verified at the IFA injector test bench. The comparison of producer-supplied data and data measured by IFA is summarized in Table 2.3. AdBlue was provided by a flexible and mobile supply and control unit.

Table 2.3: Spray characteristics

Injectors	1	2	3
	original data/measured data		
Number of holes	3	3	1
Static mass flow, kg/h	3,1/3,18	7,27/7,32	5/5,02
Injection pressure(rel.), bar	5	5	9
SMD, µm	100/84	155/178	30/38
We-number (calcul. with. SMD)	873/673	1353/1427	409/484
Spray angle, °	16/17	15/11	40/40
Injection frequency, Hz	1	1	1

2.1.3 Analytical methods

Deposits sampled from the lab test bench at KIT and engine test bench at TUW were analyzed regarding chemical composition, decomposition behavior and surface structure. Furthermore, detailed thermal and kinetic analysis was performed by various methods to study the decomposition mechanism of urea and its by-products.

A Netzsch STA 409 C instrument equipped with the thermal controller TASC 414/2 was used for thermogravimetric measurements. Representative samples were grinded and placed in a corundum crucible with an initial sample mass of 10-100 mg. The samples were heated from

40 to 700°C at a constant heating rate of 2 or 10 K min^{-1}. TGA determines the mass loss of a sample by evaporation and reactions under specified conditions and therefore gives information about the decomposition behavior. Experimental results from TGA measurements are normalized by the initial sample mass for comparison with simulation data and plotted over temperature.

HPLC analysis is used to quantify the chemical composition of derived deposits or samples taken from TGA. By this technique, a solution containing the sample is pumped through a column packed with adsorbent leading to a separation of the sample components by residence time. The samples were analyzed by a HPLC method developed in this work. A Hitachi VW12 HPLC instrument with L-2200 sampler was used for the measurements. A Waters IC-PAK Anion HC column represents the stationary phase. Downstream of the column, a L-2455 diode array detector was applied for signal analysis.

2.2 Experimental results

In the following, the results of experiments at the test benches at KIT and TUW are presented. The experiments are divided in different work packages at steady state (WP 2) and transient (WP 6) operating points to investigate deposit formation at various conditions. Furthermore, deposits and their decomposition are analyzed by TGA and HPLC method.

2.2.1 Deposit formation on lab test bench at KIT

As part of WP 2, experiments were performed at the lab test bench at KIT to create deposits. The deposit formation was studied qualitatively and quantitatively at varying operating conditions. For a gradual increase of deposit mass, three injection cycles of 40 min with a UWS mass flow of 1 g min^{-1} and a 15 min break, for water evaporation and deposit formation, in between the cycles, were conducted. The long-time injection experiments were performed at 4 different operating points OP 0 to OP 3. Furthermore, three operating points OP 4a to OP 4c were conducted with short injection time of 10s and a UWS mass flow of 4.8 g min^{-1}, which served as a basis for the simulations of the lab test bench and are further discussed in Section 2.4 . The operating conditions are listed in Table 2.4.

Table 2.4: Lab test bench operating conditions for multiple injection experiments at steady state.

OP	T_{gas} [°C]	$T_{w,st}$ [°C]	u_{gas} [m/s]	Re [-]
0	*150*	*90*	*8.6*	*11832*
1	*190*	*130*	*9.4*	*10982*
2	*280*	*175*	*11.3*	*9454*
3	*320*	*190*	*12.1*	*8903*
4a	*183*	*167*	*10.3*	*12329*
4b	*217*	*197*	*10.9*	*11444*
4c	*253*	*227*	*11.5*	*10594*

Under incident flow conditions, crystallization and deposit formation are generally observed to start at the downstream edge of the liquid film resulting in bow-shaped deposits. Nevertheless, no solid deposits are formed in the spray impact region, during the injection period. Due to urea crystallization starting at the edge of the liquid film, where the evaporation rate reaches a maximum, solidification is at first attributed to continuous liquid supply and high temperatures and second, capillary suction of liquid into the porous deposit structure is assumed to promote deposit growth.

The largest volume and mass of deposit was generated at OP 0, which result from relatively low gas and wall temperatures and assumes a composition of mainly urea crystals. As the gas temperature at OP 0 was only 150°C, it is not directly relevant to SCR application since UWS is commonly not injected below 180°C. However, this emphasizes the risk of severe deposit formation at low temperatures, yet present during start and shutdown of SCR systems. Deposits from OP 2 were produced at the downstream edge of the liquid film formed during injection and are shown in Figure 2.4. Only a small amount of solids was left after multiple injection periods. The bow-shape was similar to the deposit derived at OP 3, but the deposit covered area was larger at OP 2. This can be explained by an increased film area formed at lower temperatures. Sampled deposits feature a dense structure and partially a yellow-brownish coloring.

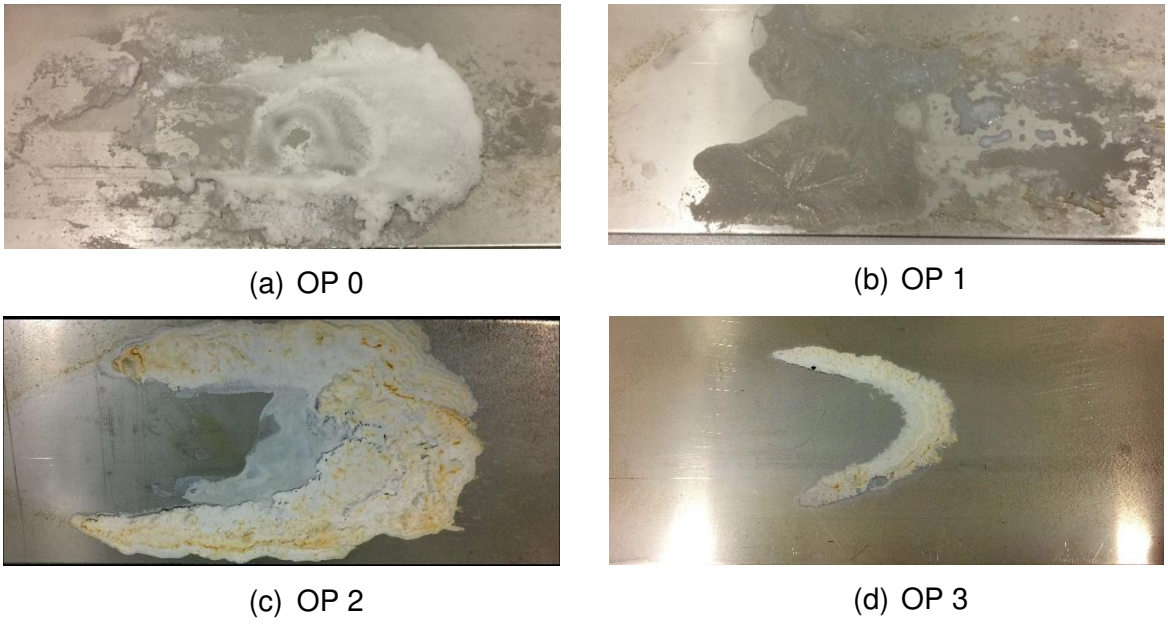

(a) OP 0 (b) OP 1

(c) OP 2 (d) OP 3

Figure 2.4: Photographs of deposits generated at different operating points. Flow direction from left to right.

Deposits derived at different operating conditions were chemically analyzed to correlate composition with responsible operating conditions. Thermogravimetric analysis gives information on the decomposition behavior of deposit samples, from which one can deduce strategies for regeneration of urea derived deposits in SCR applications. Furthermore, characteristic decomposition stages reveal the deposit composition qualitatively. For

quantitative analysis of chemical composition, additional HPLC measurements were conducted.

Results of TGA from deposits of OP 0, 1 and 4a showed a similar decomposition behavior to pure urea, indicating urea as main component. For OP 0, HPLC analysis revealed a share of 96.6 % urea and very small amounts of biuret and triuret (Table 2.5). Results from HPLC analysis showed a similar deposit composition for OP 1 and 4a. Significant amounts of biuret, triuret and cyanuric acid were found in contrast to OP 0. This explains larger mass losses during TGA for the biuret and cyanuric acid stages compared to pure urea decomposition.

The deposit derived at OP 4b was formed at temperatures around 200°C, indicating decomposition of urea and biuret. HPLC analysis furthermore revealed that urea is not present in the sample anymore, which consisted of large amounts of biuret and cyanuric acid and a considerable amount of ammelide. In contrast to pure biuret decomposition leaving a residual mass of 6 % at 600°C, 10 % of the deposit sample has remained at this temperature. The HPLC result showed the lowest recovery value for OP 4b. Both indicates the presence of further components not included in the HPLC method.

For all samples of OP 2, 3 and 4c, a large mass loss was observed to start around 260°C in TGA measurements, which is the decomposition temperature of cyanuric acid. These results were confirmed by HPLC analysis revealing a content of > 80 % of cyanuric acid and significant amounts of ammelide.

Table 2.5: HPLC analysis results of derived deposits from lab test bench at steady conditions. All results are given in %.

OP	0	1	2	3	4a	4b	4c
Urea	96.6	69.6	4.6	0.0	56.9	0.0	0.0
Biuret	0.4	16.6	trace	0.0	21.5	24.4	trace
Triuret	trace	trace	trace	0.0	5.4	0.0	0.0
Cyanuric acid	0.0	5.9	81.6	88.1	6.1	48.3	83.0
Ammelide	0.0	trace	12.2	7.1	0.8	13.6	14.3
Ammeline	0.0	0.0	1.4	trace	0	1.3	trace
Melamine	0.0	0.0	0.0	0.0	0	0.0	0.0
Recovery	97.0	90.7	99.8	95.2	90.7	87.6	97.3

The influence of the gas phase composition on deposit formation was the focus of the second experimental work package (WP 6). For operating points 0 - 3, water was added additionally to the inlet stream in concentrations of 3 – 3.5 % and the same experiments with 3x40 min injection were conducted. Besides the composition of the deposits, also the total amount of generated deposits could be compared between experiments with and without additional water. A comparison of the generated deposit mass revealed a slight trend for a decrease of

the totally deposited mass with addition of water in the exhaust gas. Especially for high temperatures, here for OP 3, additional water can help to form only very small amounts or even no deposits at all. This is explained by enhanced hydrolysis of isocyanic acid, which is a main reactant for deposits.

For further investigation of the previous results, experiments at transient conditions were conducted at the lab test bench at KIT, as part of WP 6. Experiments were conducted at an base operating point with inlet velocity of 10.7 m/s and an inlet temperature of 200°C. The addition of 1000 ppm NO seems to have no significant influence on the deposit formation, since deposit composition and total deposit mass are more or less the same. Literature considers a temperature of 350 °C and higher having an influence to the process involving NO [1,2], which was not reached in these experiments.

Subsequent the dynamic behavior of the system was investigated. After the first injection period of 40 min, the temperature was increased from 200°C to 260°C during the 30 min injection pause. At 260°C, UWS was injected for another 20 min before the system was turned off and cooled down. HPLC analysis showed that the main component is cyanuric acid, with small amounts of ammelide and undecomposed urea. The increased temperature furthermore led to an increased overall decomposition, resulting in about 50% less deposits compared to experiments at steady 200°C.

The influence of volume flow and therefore gas velocity was the focus of last two experiments, where the volume flow was decreased by 30%. Due to less film transport by shear stress the film was flowing slower downstream and more film remained at the impingement area. Splashing droplets and film spreading resulted in less deposits in the impingement area, but a lot of deposits in the channel behind the measuring cell. Only deposits from the wall of the measuring cell were analyzed, resulting in a smaller total deposit mass as expected. A high amount of triuret (31.2%) is detected for the deposits derived at with constant, low flow rates. It is expected that the triuret reaction is strongly influenced by the HNCO concentration in the gas phase. A decreased flow rate leads to a longer residence time of HNCO in the boundary layer above the film, resulting in a promoted triuret formation. For another experiment the flow rate was increased from 800 L/min to 1200 L/min after the first injection period. HPLC analysis revealed that triuret formation was decreased and deposits were comparable to operating points with constant high gas flow rate.

2.2.2 Deposit formation on engine test bench at TUW

Table 5 shows the 3 investigated steady-state operating points (OP). The exhaust gas temperatures ranged from 200 °C to 350 °C and covered operating points from the injection threshold in series applications up to the Leidenfrost regime. Additionally, the toxic ZnSe-glasses that were used for the IR-thermography would not allow temperatures above. The AdBlue mass flow was adjusted to observe a sufficient amount of solid deposits after a

measuring time of 20 min. This duration was defined as the maximum achievable simulation time with CFD. For OP 3 an additional increased mass flow was chosen to accumulate a higher amount of deposits for the following chemical analysis. No noteworthy amount of deposits could be formed at OP 1 due to the cooling of the steel plate below the critical temperature.

Table 2.6: Measurement matrix of steady-state experiments at TUW

<table>
<tr><th colspan="2">Operating points</th><th>1</th><th>2</th><th>3</th></tr>
<tr><td colspan="2">exhaust gas temperature, °C</td><td>200</td><td>275</td><td>350</td></tr>
<tr><td colspan="2">exhaust gas mass flow, kg/h</td><td>800</td><td>1000</td><td>1200</td></tr>
<tr><td colspan="2">inclination of the box, °</td><td colspan="2">18</td><td>0</td></tr>
<tr><td colspan="2">duration of a measurement, min</td><td colspan="3">20</td></tr>
<tr><td rowspan="2">injector 1,
injection rate (mg/s)</td><td>first deposits</td><td rowspan="6">no deposits</td><td rowspan="2">44</td><td>106</td></tr>
<tr><td>accumulation of deposits</td><td>132</td></tr>
<tr><td rowspan="2">injector 2,
injection rate (mg/s)</td><td>first deposits</td><td rowspan="2">40</td><td>37</td></tr>
<tr><td>accumulation of deposits</td><td>61</td></tr>
<tr><td rowspan="2">injector 3
injection rate (mg/s)</td><td>first deposits</td><td rowspan="2">132</td><td rowspan="2">418</td></tr>
<tr><td>accumulation of deposits</td></tr>
</table>

The goal of the transient experiments was the observation of deposit formation and decomposition due to a change of the thermodynamic conditions of the exhaust gas. Therefore, two strategies were investigated:

- Change of the exhaust gas temperature while maintaining a constant mass flow rate of 1000 kg/h. The deposits were generated during the first minutes of an experiment (4-7 min) under constant operating conditions. Then the exhaust gas temperature was increased with a ramp of 5-7 min to a higher value where the decomposition of the generated deposits is expected (Experiments 1-13, 18, 19 of Table 2.7).
- Change of the gas mass flow rate while maintaining a constant gas temperature. The solid deposits were accumulated during the first minutes of an experiment (5-7 min) under constant OPs and 600 kg/h exhaust gas mass flow. Then the gas mass flow rate was increased with a ramp of 12 seconds to 1000 kg/h (Experiments 14-17, 20, 21 of Table 2.7).

Table 2.7: Measurement matrix of transient experiments at TUW

injector	measur. №	accumulation of deposits				time ramp	decomposition of deposits				total duration
		Δt_1	$\dot{m}_{Ex.gas}$	$T_{Ex.gas}$	$\dot{m}_{UWS}$	Δt_2	Δt_3	$\dot{m}_{Ex.gas}$	$T_{Ex.gas}$	$\dot{m}_{UWS}$	$\Sigma\Delta t$
		min	kg/h	°C	mg/s	min	min	kg/h	°C	mg/s	min
1	1	4	1000	200	19	0	16	1000	200	0	20
	2					5	11		275		
	3					7	9		350		
	4					9	7		425		
	5	5		275	35	0	15		275	0	
	6					5	10		350		
	7									35	
	8									48	
	9					7	8		425	0	
	10									35	
	11									48	
	12	7		350	97	5	8		425	0	
	13									97	
	14	5	600	350	57	0	15	1000	350	0	
	15									57	
	16			425	141				425	0	
	17									141	
3	18	5	1000	275	69	5	10	1000	350	0	
	19	7		350	390		8		425		
	20	7	600	350	139	0	13	1000	350	139	
	21			425	404				425	0	

Figure 2.5 illustrates exemplarily the results of experiment № 21 in Table 2.7. AdBlue was injected with injector 3. The produced spray had a low area load and small droplet spectrum with low We-numbers. Due to the high initial plate temperature of approx. 360 °C a high injection rate was necessary to cool the plate below the critical wall temperature. The first liquid film was found after 120 seconds of injection, first deposits after 190 seconds. The

accumulation phase was extended to 7 minutes in order to generate a sufficient amount of deposits. Figure 2.5 a shows the video observation of the film and deposits after 7 min. In the left picture, the footprint of the spray and the liquid film can be observed. Shear stress from the exhaust flow pushed the film downstream to plate regions with higher temperatures. There, deposits were created wherever the film stagnated. Subsequently the UWS injection was stopped and the exhaust mass flow rate was rapidly increased to 1000 kg/h as shown in Figure 2.5 b. The plate temperature in the deposition area rose by approx. 140 °C due to a higher heat transfer from the exhaust gas and the lack of water evaporation from AdBlue. Consequently a fast deposit decomposition was observed. Nevertheless, a noticeable amount of deposit was found at the end of the experiment. The HPLC analysis, which was carried out at KIT, showed that the remaining deposits consisted of 64 % ammelid and 30 % ammelin. The residual was an unknown substance.

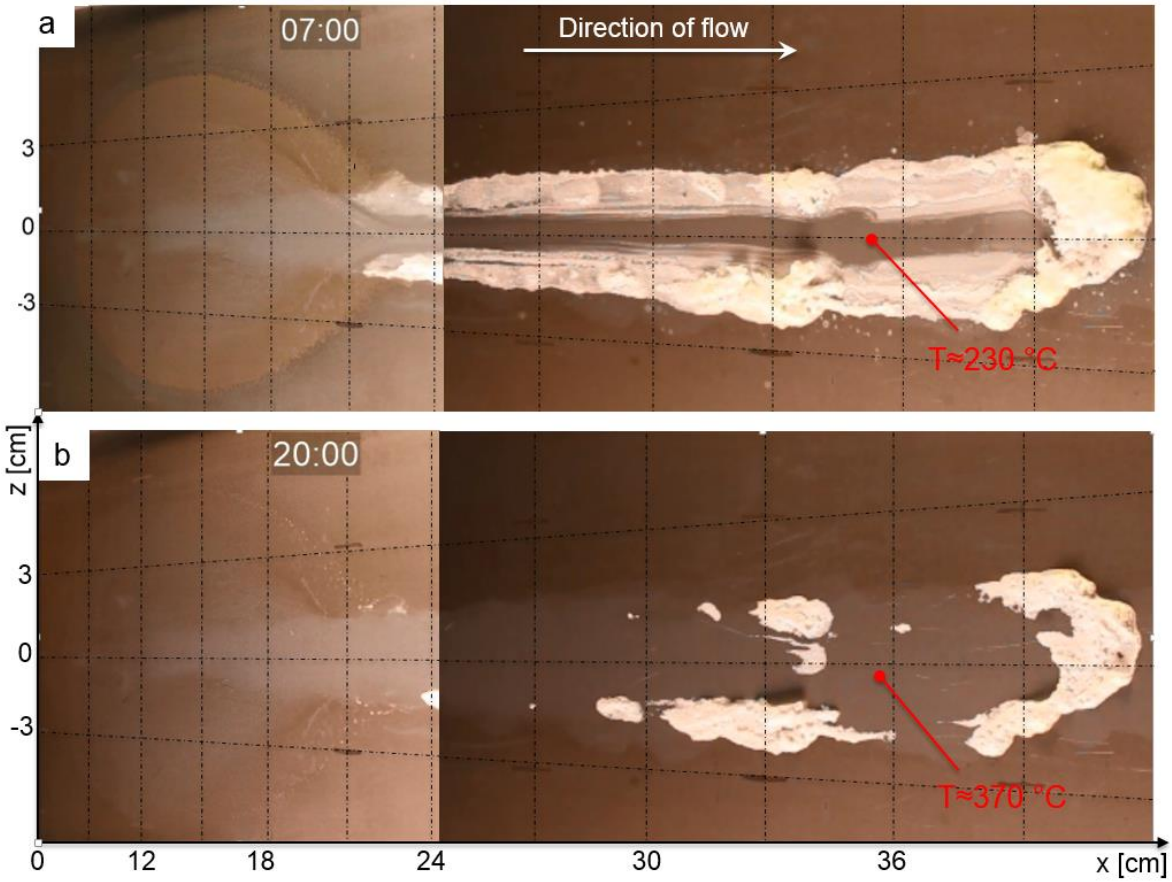

Figure 2.5: Results of the measurement № 21. (a) solid deposits at the end of the accumulation phase, (b) solid deposits at the end of the decomposition phase.

2.2.3 Thermogravimetric decomposition of urea and its by-products

Thermogravimetric analysis was used to study the decomposition behavior of urea and its by-products in detail. It delivered data on decomposition temperatures and characteristic stages and could further be used for qualitative conclusions on the sample composition when analyzing urea deposits.

Figure 2.6 shows TGA results for urea and all relevant by-products included in this study. Here, a heating rate of 2 K min^{-1} was applied for an initial sample mass of 5 mg.

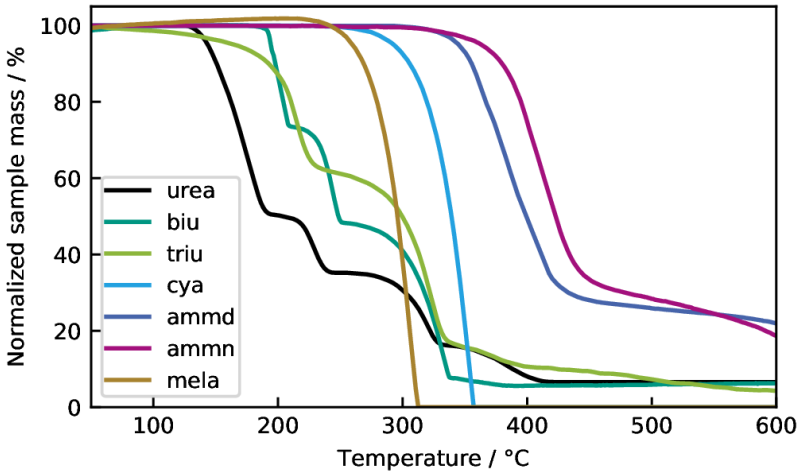

Figure 2.6: Thermogravimetric decomposition of urea and its by-products. Experiments are performed with an initial sample mass of 5 – 6 mg in the cylinder-type crucible using a heating rate of 2 K min^{-1}.

Urea decomposition starts at 133°C and is followed by biuret and triuret decomposition producing cyanuric acid and ammelide. Decomposition of cyanuric acid and ammelide is initiated at 250°C and 360°C, respectively. Ammelide is assumed to react to ammeline, which starts decomposing subsequently. Ammeline is proposed to react to melamine by Bernhard et al [3]. In other works, melamine was only found to be present in small amounts at 250°C. Experiments shown in Figure 2.6 revealed the start of melamine decomposition at 250°C. Since it was fully decomposed at temperatures above 300°C, melamine, which is formed during ammeline decomposition, is assumed to decompose instantaneously.

2.3 Kinetic and CFD modeling

In the following, setups for CFD simulation and the applied physics are described. 0D simulations of the urea decomposition kinetics were performed using a kinetic model adapted from Brack et al. [4]. Furthermore, the decomposition kinetics were integrated into the 3D CFD simulations.

2.3.1 Modeling Physics

The numerical modeling of deposit formation and decomposition was carried out with the CFD code StarCCM+ v13.06. Several model modifications were made on the spray and impingement models in order to fit the experimental observations:

- A Cunningham correction factor was introduced in the spray model in order to correlate the simulated droplet trajectories with the observations from high-speed imaging.
- The critical wall temperature in the Bai-Onera impingement model was expressed as a function of the We-number.

- The droplet deformation in the Wruck heat transfer model was adjusted with the Akao correction in order to correlate the simulation results with the IR-thermography measurements.

After receiving a good correlation of the spray and film simulation with the experiments at the engine test bed the modelling of the time scales became the focus of the work. The numerical prediction of deposit formation and decomposition required modeling of physical and chemical processes with different time ranges:

- Wall cooling, film formation, growth and decomposing of deposits - time range of minutes.
- Chemical reactions - time range of milliseconds.
- Spray propagation and droplet impingement - time range of microseconds.

With regard to the simulation wall time, the modeling of the spray propagation and the droplet impingent is most critical. The presence of the Lagrangian phase in the simulation domain limits the reasonable simulation time step to the range of approx. 0.1-0.7 ms and increases the modelling effort proportionally to the injection time. Moreover, these processes are periodic and thus are repeated many times until the simulation of the deposit formation or decomposition is completed.

In order to overcome the issues described above and thus accomplish the modelling of deposit formation and decomposition in typical time ranges, an injection source approach was developed. In this approach the numerical parcels that represent the spray were substituted by source terms of mass, momentum and energy that were directly applied to the film and gas phase. The source terms for both phases were calculated simultaneously during a single injection event. These preparatory simulations were carried out for diverse wall temperatures and the source terms were stored for the use in the following transient simulation with the long time durations. One setup could be used as long as the operating conditions remained constant, i.e. as long as the spray deflection and the impingement positions of droplets were not changing. When simulating transient operating conditions the source terms must be updated continuously with the specific combination of spray and exhaust mass flow.

With this approach, it was possible to increase the simulation time step to a range of 5-10 ms. Furthermore, the computing time of a simulation time step was reduced by approx. 25 %. Even with detailed chemistry simulation times of 45 s/day was achieved with one computer core per 30.000 cells. That is well beyond typical capabilities.

Figure 2.7 illustrates a mass and impingement heat source calculated with the injector 1 at OP 3 (see Table 2.6) and applied to the shell region of the surface. Due to a high initial temperature of the impingement plate above Leidenfrost temperature, no liquid film deposition occured at the beginning and only the heat source was applied to the film region where the AdBlue droplets impinge on the surface (< 0 because the plate is cooled), see Figure 2.7a left. In the

right picture the absence of any liquid deposition due to the high surface temperature is shown. After 60 s the plate temperature fell below the critical wall temperature due to the permanent cooling from the AdBlue injection. Now, the mass sources of water and urea were activated and the cooling was calculated as heat conduction between the liquid film and surface, see Figure 2.7b right. Therefore, in Figure 2.7 b left the heat sources are zero at the locations where liquid mass was applied.

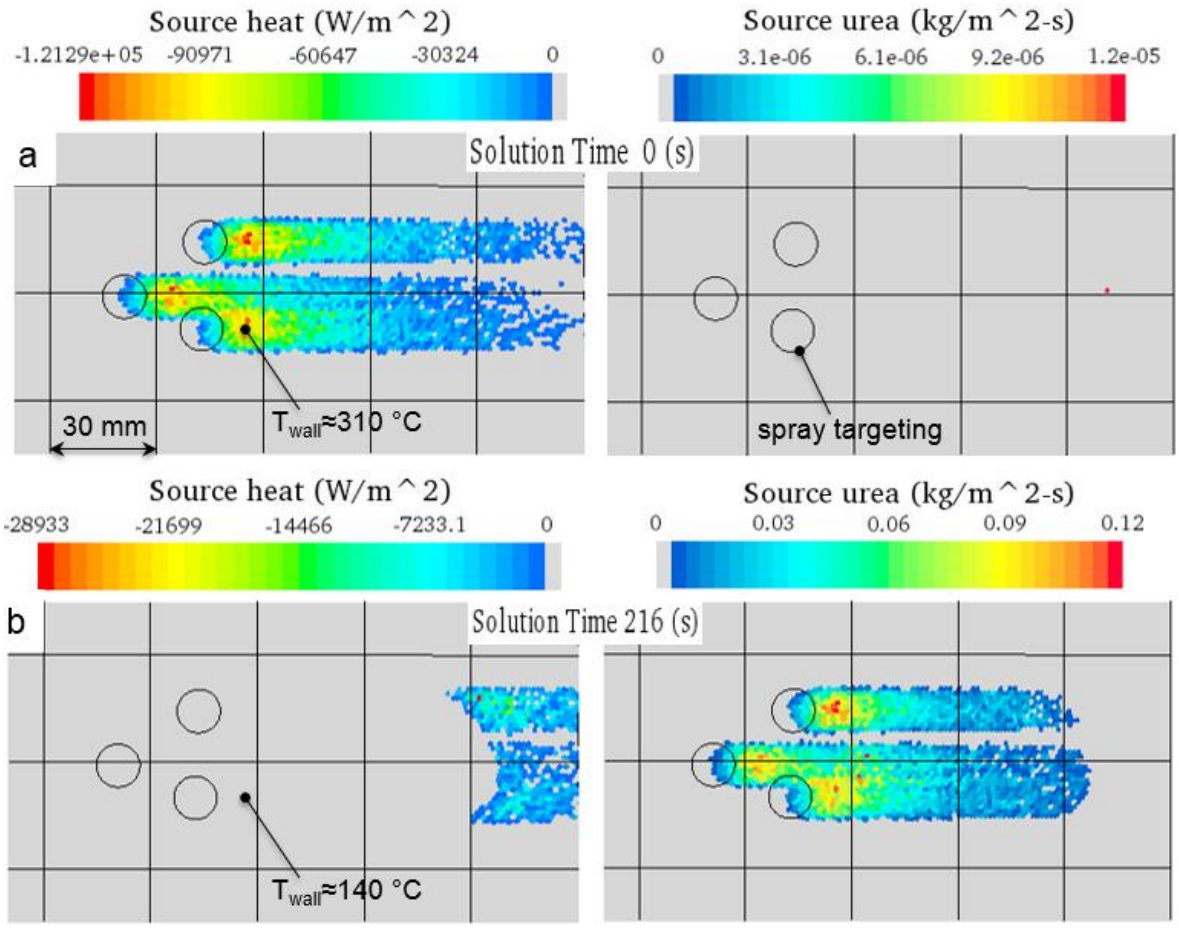

Figure 2.7: Impingement heat and urea mass source at the beginning of the simulation (a) and after 216 second of the solution time (b). OP 3, injector 1, injection rate 132 mg/s.

The third part of the simulation physics was the implementation of the detailed chemical solution provided by DETCHEM, the in-house chemistry solver at KIT, which is presented in the following.

2.3.2 Urea decomposition model

For simulation of urea decomposition an adapted kinetic model proposed by Brack et al. [4] was used. For time-dependent simulations of the chemical kinetics the numerical simulation software DETCHEM^{TM} was applied [5].

The MPTR (Multiple Phase Tank Reactor) code of the DETCHEM^{TM} software package [5] was used, which represents a 0D batch-type reactor model containing a gaseous phase and multiple condensed phases. A sketch of the DETCHEM^{MPTR} model can be seen in Figure 2.8.

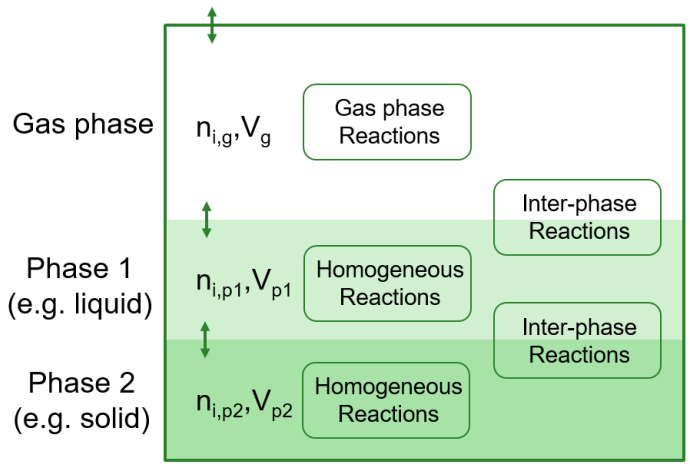

Figure 2.8: Sketch of the DETCHEM^{MPTR} model.

The reactor model consists of a set of species S_i, which are grouped into sets of phases P_j. Each species belongs to exactly one phase, i. e. a phase transition of a chemical substance is handled by two different species. Each species is associated with thermodynamic data in form of the NASA polynomials [6], by which molar heat capacity $c_{p,i}$, molar enthalpy $H_{m,i}$ and molar entropy $S_{m,i}$ are computed. The concentrations are expressed locally with respect to the corresponding phase, i. e. $c_i = n_i/V_j$. The reaction rates are mostly given in terms of Arrhenius expressions. The batch-type reactor model consists of conservation equations for species and enthalpy. More information about the MPTR model and kinetic development can be found in Tischer et. al [7].

2.3.3 Integration of kinetic model into CFD

In order to use the developed reaction mechanism of urea decomposition presented in [4] in the CFD simulation, it was necessary to implement the thermophysical properties of all relevant species. Further, kinetic data of urea decomposition and the MPTR algorithm had to be integrated to the CFD code.

For integration of urea decomposition reactions a user code was developed, which contains the numerical and kinetic algorithm applied in the DETCHEM^{MPTR} code. User codes enable the development of user defined functions that can be called by the different submodels in StarCCM+. The user code was written in C. The user function could be called from the chemistry sub-model for calculation of the species production rates. Respective production rates (in $\mathrm{mol\,m^{-3}\,s^{-1}}$) were calculated in the CFD code from the ω values by summation and division by the phase mass. Concentration, pressure, temperature, film thickness, cell area and time step data were transferred to the user code for each liquid film cell in each time step via the established interface. Based on these data and the implemented MPTR algorithm, reaction rates were calculated by the user code, which were delivered to the chemistry model in StarCCM+. Species concentrations in the liquid film were updated. Gas-liquid equilibria and all other physical processes were then calculated by physical models in StarCCM+.

2.4 Simulation results

The applied models and the integration of urea decomposition kinetics were validated for various conditions by simulations of thermogravimetric analysis and experiments at lab test bench and engine test bench.

2.4.1 Simulation of thermogravimetric decomposition

Thermogravimetric decomposition of different samples in the cylinder crucible were simulated with a heating rate of 10 K min^{-1} in order to reduce total simulation time. Results were compared to experiments of identical boundary conditions in terms of sample mass loss over temperature. Furthermore, 0D simulations were performed in DETCHEM^{MPTR} to evaluate the implementation of the kinetic model.

As an example the thermogravimetric decomposition of UWS is shown in Figure 2.9, comparing the experimental and the numerical results from 0D and 3D.

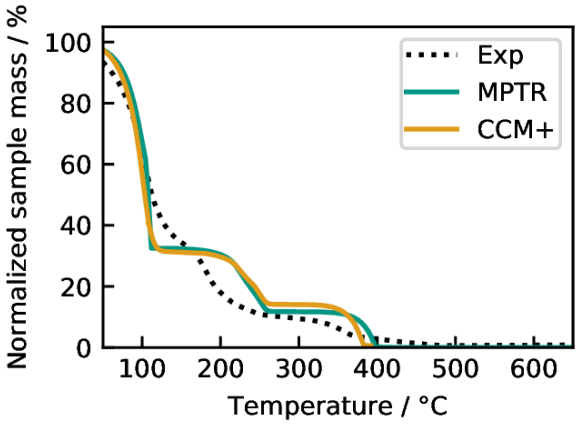

Figure 2.9: Thermogravimetric decomposition of 27.5 mg urea water solution using a heating rate of 10 K min^{-1}. Comparison of experimental data with results from 0D simulation in DETCHEM^{MPTR} and 3D simulation in StarCCM+.

Results on the decomposition of urea and its by-products were used to evaluate the implementation of the DETCHEM^{MPTR} algorithm and the corresponding kinetic model into the CFD simulation in StarCCM+. The test case of thermogravimetric analysis showed a good agreement of simulation results with experimental data. Slight deviations to experimental results originated from the kinetic model and might be improved by further developing urea decomposition kinetics. Differences between DETCHEM^{MPTR} and StarCCM+ simulations were observed for cases including interface reactions and evaporation. For the actual purpose of simulating deposit formation in flow setups and real applications, high gas flow rates above potential liquid films are expected to reduce this effect.

2.4.2 Simulation of Lab test bench

Experiments from the lab test bench at KIT were simulated for the purpose of testing the implementation of chemical kinetics in the CFD model to realistic conditions. Therefore the

modeling approach was used to simulate short-term injection experiments to remain in feasible computational times.

As a result of the implemented kinetic model for urea decomposition, the evolution of by-products in the liquid film could be tracked temporally and locally. In the beginning of the simulations with injection of UWS the resulting film consisted of mainly water and aqueous urea. Since water is evaporating, the aqueous urea starts to form liquid urea. With decreasing film and wall temperature, due to spray/wall heat transfer and evaporative cooling, the liquid urea starts to solidify. Figure 2.10 shows the spatial distribution of by-products formed from urea at OP 1 after 1 s.

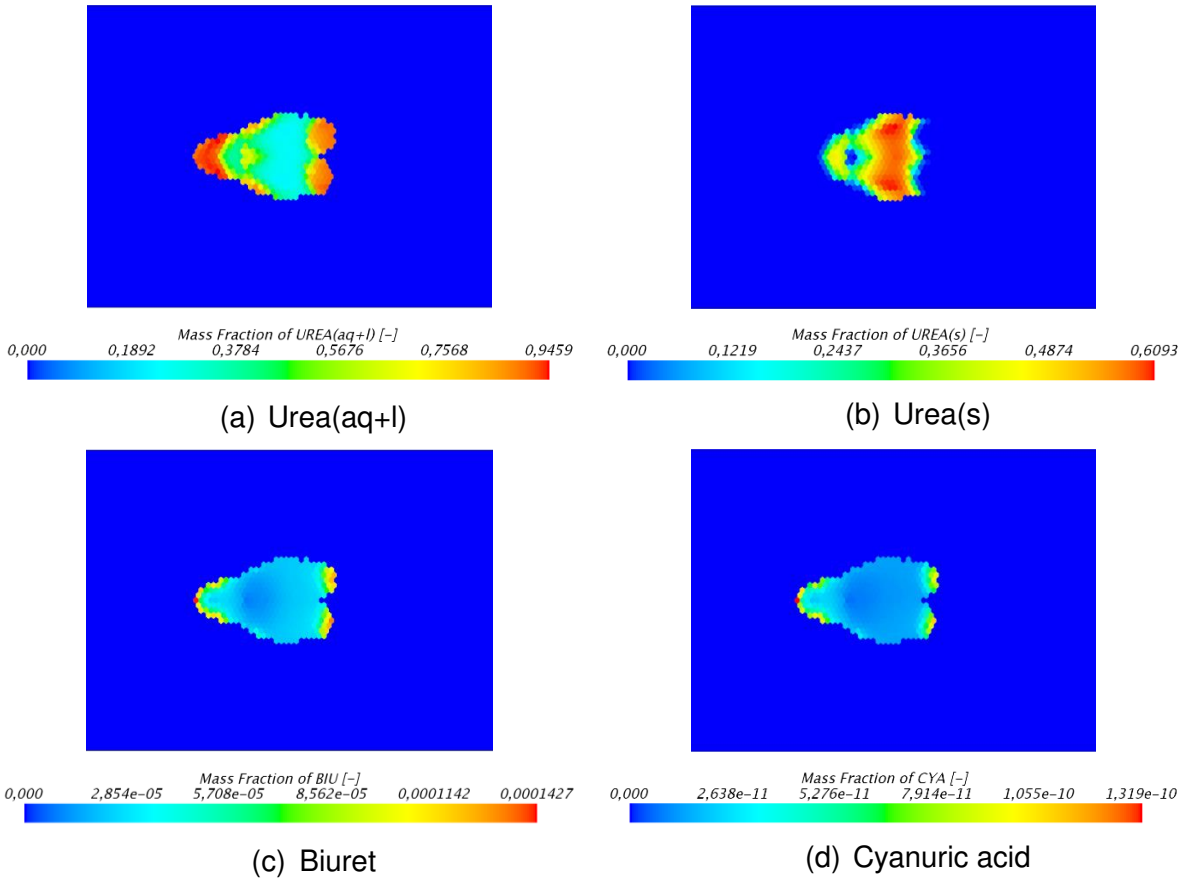

Figure 2.10: By-product formation from liquid urea at OP 1 after t=1s.

After 1 s urea had hardly decomposed what resulted in a large amount of aqueous, liquid and solid urea in the film. Molten urea was observed along the edge of the solid urea bulk and further downstream as it was transported by shear stresses due to its low viscosity and was formed due to higher temperatures. From the liquid urea melt, small amounts of solid by-products were formed by the reactions implemented through the user kinetic model. At temperatures of 185°C urea reacted to biuret, which in turn reacted to cyanuric acid.

During the injection of 10 s more and more water and aqueous urea remained on the surface. Due to the decreased wall temperatures and evaporation of water the solubility limit of urea was reached and solid urea was formed out of the film. As already seen in Figure 2.10, liquid

urea was formed mainly at the edge of the film. After the injection, water evaporated very fast and the film consisted of mainly solid urea. With reaching 30 s of the experiment, the film was already heated above the melting point of urea again and the liquid film flew downstream the channel. In the liquid urea melt and due to increased temperatures, the by-product formation started to form considerable amounts of biuret, cyanuric acid and ammelide which further limits the transport of the film, due to increased viscosity.

Comparison of numerical with experimental data was only partially feasible, because experiments with short time injection of 10s produced too few deposits for a further analysis. Table 2.8 compares experimental data of deposit composition at OP 4b after a long-term injection of 3 x 40 min with simulation results derived in StarCCM+ at different (physical) time instants. The experimental analysis by HPLC revealed the ammeline content in addition to other by-products. Since ammeline was not considered in the applied kinetic model, the ammeline content remained zero for the simulation. Results showed that the experimentally measured deposit composition could not be reproduced by the simulation for a physical simulation time of 18 min. However, some conclusions can be drawn from the evolution of the deposit composition in the simulation over time.

Table 2.8: Experimentally determined composition for deposits derived at OP 4b in comparison to simulation data resulting after different physical time instants and deposit mass divided by total injected mass.

Component		Experiment	StarCCM+ 3D		
	%	3 x 40 min	4 min	8 min	18 min
Urea		0	57.47	5.9	0
Biuret		24	41.32	86.1	69.9
Triuret		0	0.004	0.05	0.4
Cyanuric acid		48.3	0.08	1.0	9.2
Ammelide		13.5	1.1	6.8	20.5
Ammeline		1.3	0	0	0
Recovery		87.6	100	100	100
Deposit Mass / Injected Mass		1.66	9.6	6.0	3.6

Table 2.8 demonstrates further decomposition of urea with time. After 18 min urea had completely decomposed and the resulting deposit mainly consisted of biuret. Biuret further reacted to cyanuric acid and ammelide. As the temperatures at OP 4b was above the biuret decomposition point, biuret was expected to be gradually decomposed to ammelide and cyanuric acid with time. Consequently, the deposit composition in the simulation was assumed to approach the experimentally determined values.

2.4.3 Simulation of Engine test bench

. In the following, selected simulation results of the engine test bench with adapted and validated submodels will be presented to demonstrate the capabilities of the modelling approach.

Figure 2.11 shows the positions of the simulated and observed liquid film and solid deposits after 216 s experimental time.

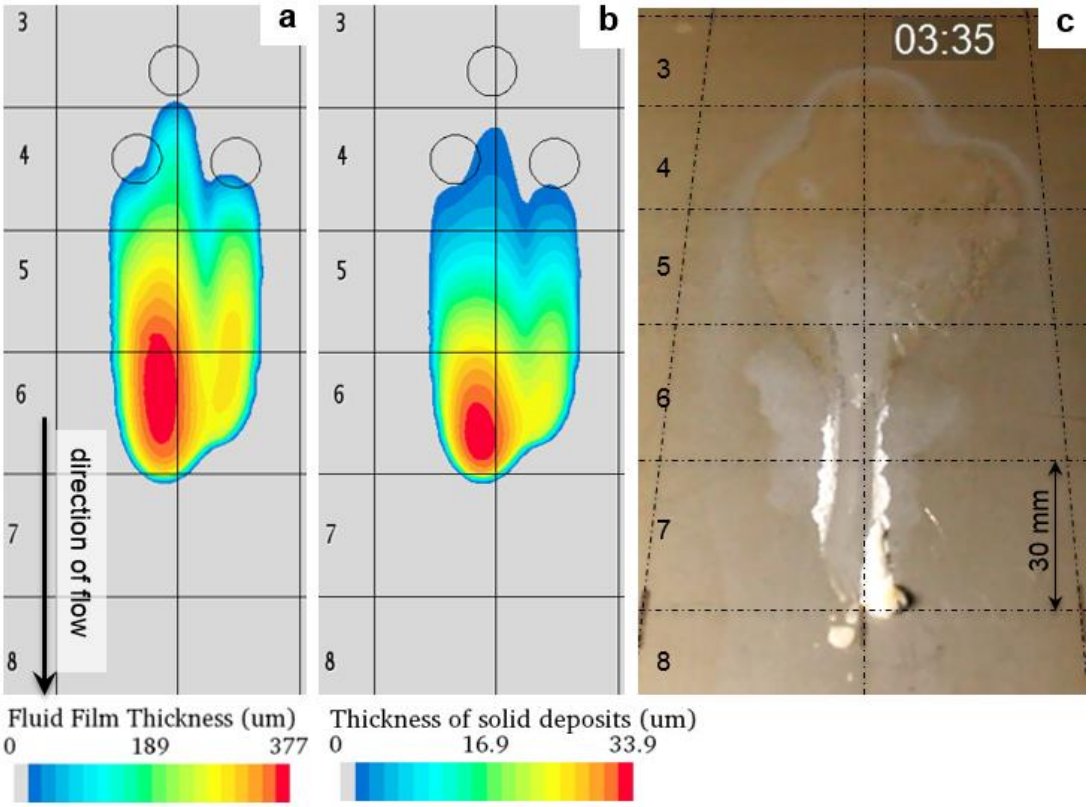

Figure 2.11: Film and deposit formation on the impingement plate. a – simulated film thickness, b – simulated thickness of solid deposits, c – experimental result. OP 3, injector 1, injection rate 132 mg/s.

Generally, a reasonable agreement can be observed. In comparison to the measured data, the front of the modelled liquid film was approx. 30 mm closer to the initial foot print of the spray. This difference is mainly caused by the delay of 20 s between the occurrence of the first film in the simulation compared to the experiment. Nevertheless, the film velocity (approx. 1 mm/s) was well predicted. Furthermore, most deposits were located close to the front of the liquid film, what correlates well with the experimental data. The film temperature at this area was significantly higher than that at the position of the initial foot print. That accelerated the side reactions of the urea decomposition and led to a faster formation of solid deposits

Figure 2.12 illustrates the comparison of the simulated plate temperature drop with the IR-thermography measurement at the bottom side of the impingement plate. The simulated temperature drop in the area of the initial foot print was in good agreement with the measured

data. The cooling area downstream of the initial foot print was slightly overestimated due to a wider front of the liquid film.

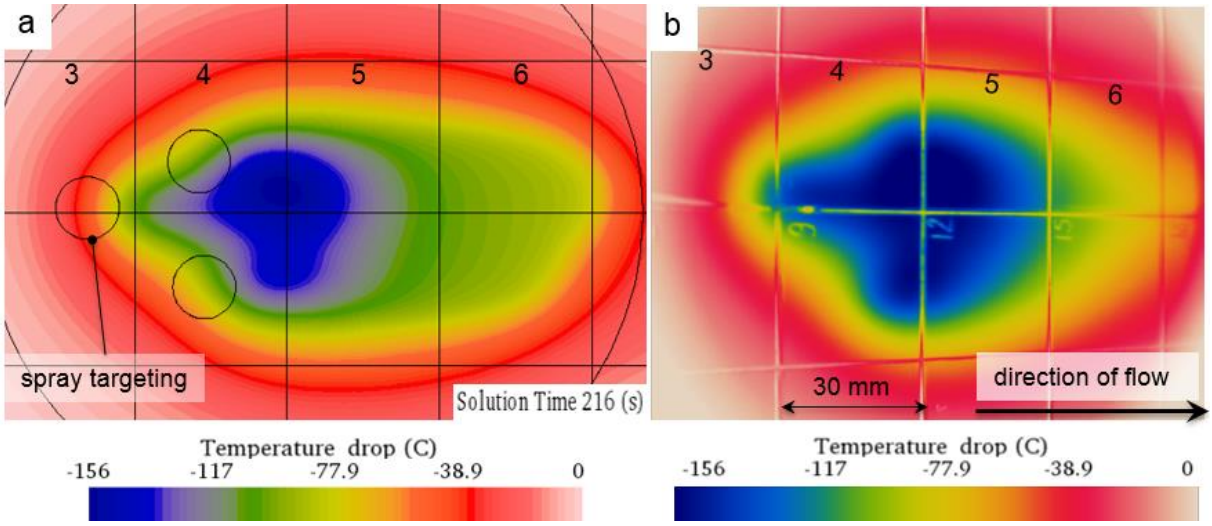

Figure 2.12: Simulated and measured temperature drop at the bottom side of the impingement plate. OP3, injector 1, injection rate 132 mg/s.

The formation of the film components is plotted in Figure 2.13. The blue and red lines represent the AdBlue (urea-water-solution, UWS) and solid deposits, respectively.

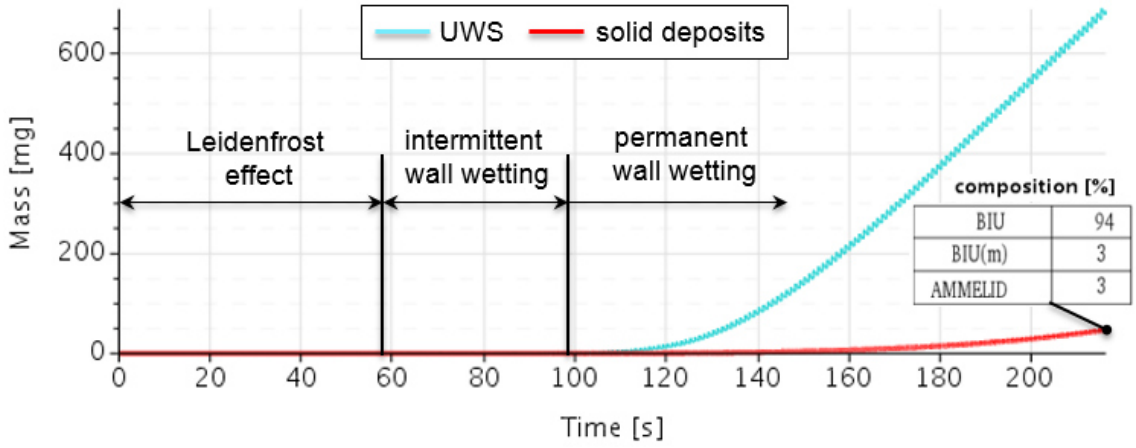

Figure 2.13: Simulated mass of UWS and solid deposits. OP3, injector 1, injection rate 132 mg/s.

The following successive physical effects can be distinguished in the diagram: Leidenfrost effect, intermittent and permanent wall wetting. A fast deposit formation is observed after the liquid film left the area of the initial foot print (approx. 160 s). During the simulation time of 216 s, 52 mg of solid deposits were accumulated in the film. The main component of simulated deposits was biuret. In contrast to that, the real deposits consisted mainly of cyanuric acid. These differences may refer to some inaccuracy of the kinetic model of urea decomposition as well as to fact that the simulation time is limited to 216 s.

Figure 2.14 illustrates the simulated and measured results of the transient experiment №5 (see Table 2.7).

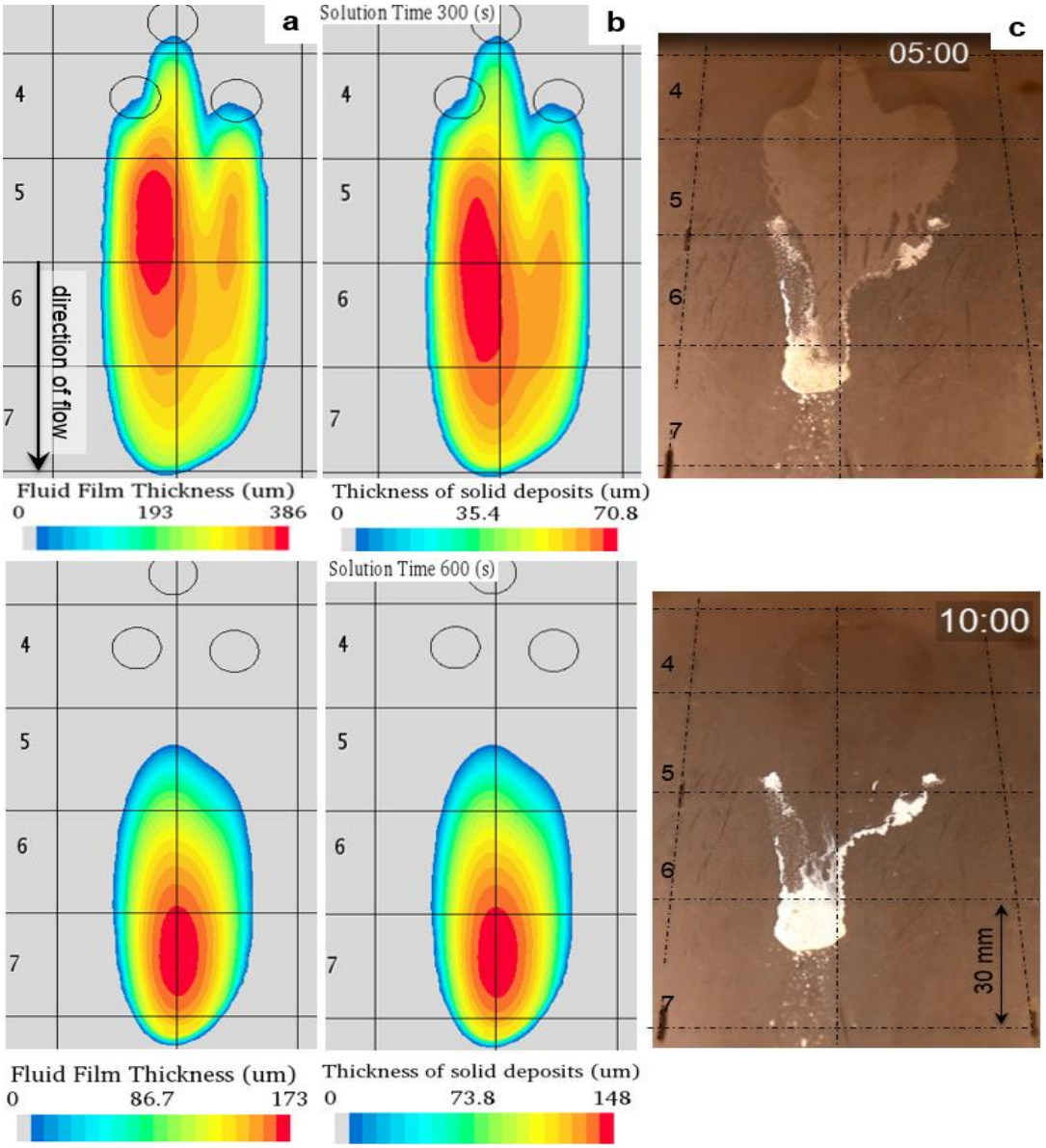

Figure 2.14: Film and deposit formation on the impingement plate. a – simulated film thickness, b – simulated thickness of solid deposits, c – experimental result. Transient measurement №5 (Table 2.7).

The liquid film and the solid deposits were accumulated during the first part of the experiment, i.e. 300 s. The film propagation and the position of the solid deposits were well predicted. The width of the liquid film downstream the initial foot pint was overestimated. Further research work on critical fluid properties like the surface tension of liquid urea in dependency of the temperature may be therefore necessary. After 300 s the UWS injection was stopped. Hence, the film temperature started to rise and a fast film evaporation was observed. The further propagation of the film was inhibited due to a high viscosity of the solid deposits dissolved in the film.

Figure 2.15 shows the comparison of the simulated and measured temperature drop at the end of the first part of the experiment. Once again, the temperature drop in the area of the

initial foot print was in a good agreement with the measured data. Due to a wider front of the film, the cooling area of the film downstream the initial foot print was overestimated.

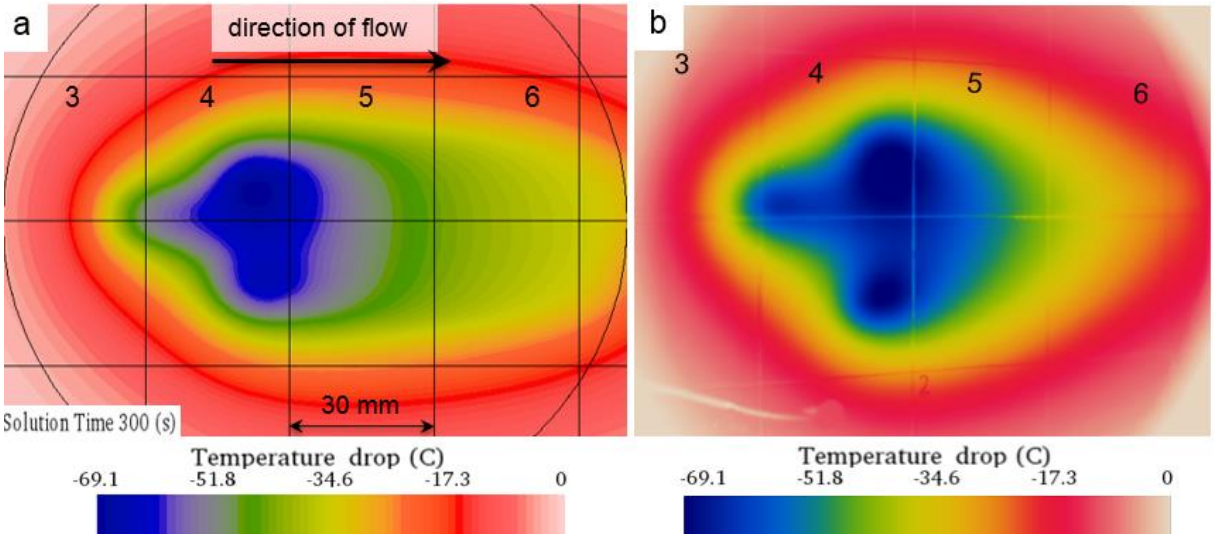

Figure 2.15: Simulated (a) and measured (b) temperature drop at the bottom side of the impingement plate. Transient measurement Nº5.

The formation and decomposition of the film components is plotted in Figure 2.16. Due to a low initial plate temperature, permanent wall wetting is observed.

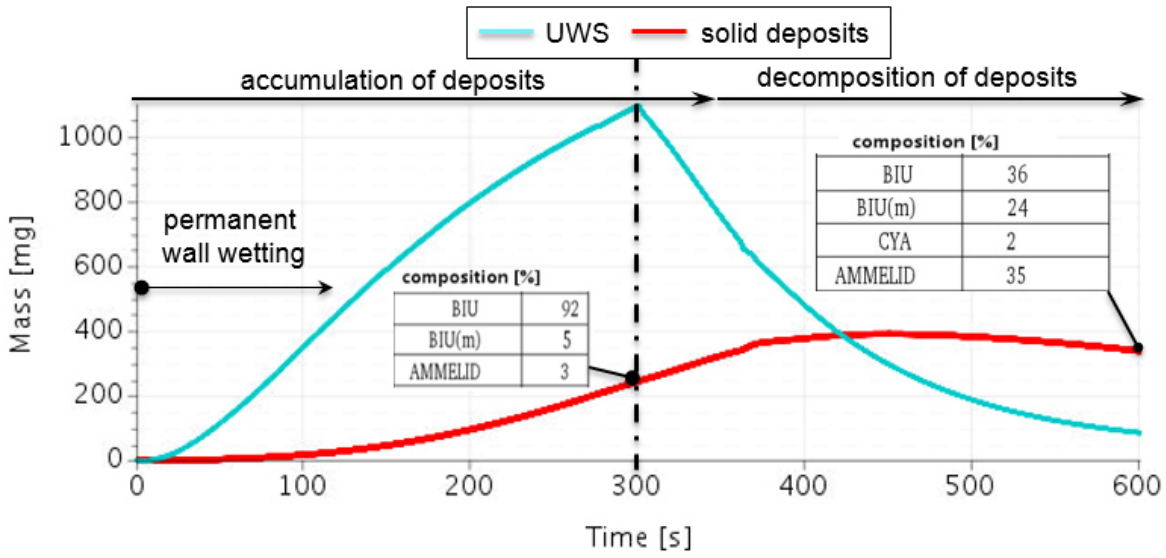

Figure 2.16: Mass of UWS and solid deposits. Transient measurement Nº5.

A fast deposit formation occurred after the liquid film left the area of the initial foot print (approx. 80 s.). The main component of simulated deposits at the end of the first part of the experiment was biuret (92 %). After 300 s the film temperature started to rise what caused the decomposition of biuret into ammelid (35 %), biuret matrix (24 %) and cyanuric acid (2 %). In contrast to that, the real deposits at the end of the experiment consisted mainly of the cyanuric acid.

3 Summary and Outlook

In the framework of this project, detailed experimental and numerical investigations on multiphase, reacting flows in SCR systems were carried out. Consequences from urea water solution dosing into the hot exhaust, such as extensive spray/wall interaction and resulting solid deposit formation were studied.

The goal of the project was the fundamental understanding of chemical and physical processes during UWS injection and deposit formation in SCR exhaust systems. Experiments were conducted on lab scale at KIT and on an engine scale at TUW in order to create a better understanding of spray/wall interaction, impingement heat transfer, the formation of wall film and solid deposits. Therefore, test benches were set up and advanced measuring techniques were applied in order to investigate the relevant physical and chemical processes.

Measurements at steady-state and transient operating conditions were carried out in order to provide a comprehensive experimental database that provides fundamental knowledge and allows the validation of numerical models. The whole process chain from spray formation, droplet impingement on a hot surface, film formation and wall cooling was investigated with high-speed and video imaging, laser diffraction and IR-thermography. The dimensions of the formed deposits were measured and both decomposition kinetics and chemical composition were analyzed in detail and discussed together with measured reference data of urea and its by-products. Experiments showed a decrease of the total mass of deposits sampled from the test rig for a multiple injection dosing strategy of up to 60 %. Due to the partial solubility of the formed by-products in UWS, solids were re-dissolved in the injected UWS leading to further decomposition.

Detailed chemical analyses of deposits derived at different operating conditions showed that the chemical composition of by-products formed from urea decomposition can be deduced from the decomposition stages of urea water solution identified by TG analysis and the decomposition mechanism of urea proposed by Brack et al. [4]. Hence, deposit composition is mainly dependent on temperature. Deposit composition was investigated by both TGA and HPLC. HPLC results were correlated to the respective decomposition stages detected by TGA. Deposits created at high temperatures were observed to require increased temperatures for decomposition. For deposits derived at temperatures below 200°C, urea represented the main component. With increasing temperature, the portion of urea was decreasing. Deposits derived in the temperature range of 200-250°C mainly consisted of biuret and cyanuric acid. Cyanuric acid and ammelide were the main components for deposits derived at higher temperatures. However, this study proposes the existence of further chemical compounds besides well-known by-products formed by urea reactions even at low temperatures. TGA experiments revealed portions of up to 10 % of these highly temperature resistant substances. Results showed that particularly biuret, triuret and ammelide decomposition produces large portions of

residues stable up to 700°C. In contrast to existing literature stating high temperature operation as less critical with regard to deposit formation [8–12], these components were found to represent a high risk of deposit accumulation without a possible regeneration.

Based on kinetic data from thermogravimetric analysis and thermodynamic considerations, the urea decomposition model proposed by Brack et al. [4] was extended and kinetically adapted. The numerical model setup for simulating decomposition represented a 0D batch-type reactor including multiple condensed phases. By implementation of interface reactions, the effect of variable surface-to-volume ratios could be reproduced by the model. An increase of interfacial area was observed to positively affect urea decomposition in terms of solid by-product formation. Moreover, this model was implemented to a 3D CFD simulation by user coding. The CFD model included the turbulent two-phase flow, spray/wall interaction, film formation and evaporation. For the first time, relevant physical and chemical phenomena in the mixing section of SCR system were predicted by a comprehensive model. The implementation routine was tested by simulations of thermogravimetric decomposition of urea and various by-products. Results showed an excellent agreement of the predicted decomposition kinetics compared to the 0D model and experimental data.

Furthermore, the comprehensive modeling approach was applied to CFD simulations of turbulent exhaust flow on an engine test bed. Modifications and enhancements were developed for the droplet drag force model, the Bai-Onera impingement map and the Wruck heat transfer model based on the experimental database from the engine test bench. A good agreement was obtained between measurements and simulation with respect to spray impingement, film formation and material cooling due to heat conduction and water evaporation from the UWS. For the first time, local by-product formation from the liquid film could be investigated in the framework of a CFD simulation. The results were in a reasonable agreement with the chemical analysis of the deposits from the test bed. However, further improvements and validation will be necessary in the future.

Apart from the chemical and physical models, a numerical method based on the source term approach was implemented in order to substantially speed up the CFD simulations. With the source term methodology it was possible to pre-tabulate the sources of mass, momentum and energy for an injection event at given thermodynamic boundary conditions and substitute the spray simulation with these source terms in the transient simulations that covered time durations of several minutes. A considerable acceleration of the CFD simulation was reached that enabled the calculation of sufficiently long time intervals to take the chemistry of deposit formation into account. This project therefore provides a feasible numerical implementation method for chemical kinetics of urea decomposition and demonstrates the capabilities of the developed modeling approach. Apart from StarCCM+, which was used in this project, the workflow can be applied to other commercial CFD codes.

A revised kinetic model for urea decomposition was presented which showed an improved agreement between experiments and the numerical simulation of TGA. Future studies could include these kinetics to the CFD simulations of systems with UWS injection to achieve a better agreement with experimental data in terms of the decomposition kinetics.

Though the new simulation workflow provides a comprehensive approach to deposit modelling, it is limited by the boundary layer approach of the fluid film model and therefore restricted to small film and deposit heights. As a result it is not possible to simulate growing deposits that restrict the free flow area. Furthermore, solid deposits have to be modeled as pseudo-liquid species, because of a lack of possibility to include solid species into the fluid film model. Another restriction is the limited access to several values, such as gas phase concentrations, for the reactions in the fluid film. It is proposed to expand the fluid film model with suitable solutions for the mentioned problems to increase the possibilities, but also the accuracy of the presented workflow.

Future studies should investigate the influence of different surface properties, structures and roughness on the impingement process and deposit formation, which are observed to play a big role in real applications. In addition, the effect of catalytic coatings is of high interest. A fundamental study on the morphology of created deposits can help to understand the formation and decomposition process of deposits. If liquid film accumulates droplets may strip and re-impinge further downstream of the exhaust system resulting again in deposit formation. Investigations on the stripping process and the extension of the source term methodology to these scenarios should be addressed in the future.

Overall, the presented work in this project delivers a good basis for further investigations of the UWS injection and deposit formation to enhance the limits of SCR systems and ensure lower NO_x emission in the near future.

4 References

[1] E. Seker, N. Yasyerli, E. Gulari, C. Lambert, R.H. Hammerle, NOx reduction by urea under lean conditions over single step sol–gel Pt/alumina catalyst, Applied Catalysis B: Environmental 37 (2002) 27–35.

[2] J.H. Baik, S.D. Yim, I.-S. Nam, Y.S. Mok, J.-H. Lee, B.K. Cho, S.H. Oh, Control of NO x Emissions from Diesel Engine by Selective Catalytic Reduction (SCR) with Urea, Topics in Catalysis 30/31 (2004) 37–41.

[3] A.M. Bernhard, D. Peitz, M. Elsener, A. Wokaun, O. Kröcher, Hydrolysis and thermolysis of urea and its decomposition byproducts biuret, cyanuric acid and melamine over anatase TiO2, Applied Catalysis B: Environmental 115-116 (2012) 129–137.

[4] W. Brack, B. Heine, F. Birkhold, M. Kruse, G. Schoch, S. Tischer, O. Deutschmann, Kinetic modeling of urea decomposition based on systematic thermogravimetric analyses of urea and its most important by-products, Chemical Engineering Science 106 (2014) 1–8.

[5] O. Deutschmann, S. Tischer, S. Kleditzsch, V. Janardhanan, C. Correa, D. Chatterjee, N. Mladenov, H.D. Minh, H. Karadeniz, M. Hettel, V. Menon, A. Banerjee, DETCHEM Software package, 2018, www.detchem.com.

[6] A. Burcat, Burcat's Thermodynamic Data: Thermochemical species in polynomial form, www.burcat.technion.ac.il.

[7] S. Tischer, M. Börnhorst, J. Amsler, G. Schoch, O. Deutschmann, Thermodynamics and reaction mechanism of urea decomposition, Physical Chemistry Chemical Physics (2019).

[8] V.O. Strots, S. Santhanam, B.J. Adelman, G.A. Griffin, E.M. Derybowski, Deposit Formation in Urea-SCR Systems, SAE International Journal of Fuels and Lubricants 2 (2009) 283–289.

[9] H. Smith, T. Lauer, M. Mayer, S. Pierson, Optical and Numerical Investigations on the Mechanisms of Deposit Formation in SCR Systems, SAE International Journal of Fuels and Lubricants 7 (2014) 525–542.

[10] S.Z. Bai, S.G. Lang, K.P. Yuan, Y. Liu, G.X. Li, Experimental Study of Urea Depositions in Urea-SCR System, Advanced Materials Research 937 (2014) 74–79.

[11] W. Brack, B. Heine, F. Birkhold, M. Kruse, O. Deutschmann, Formation of Urea-Based Deposits in an Exhaust System: Numerical Predictions and Experimental Observations on a Hot Gas Test Bench, Emission Control Science and Technology 2 (2016) 115–123.

[12] S. Sadashiva Prabhu, N.S. Nayak, N. Kapilan, V. Hindasageri, An experimental and numerical study on effects of exhaust gas temperature and flow rate on deposit formation in Urea-Selective Catalytic Reduction (SCR) system of modern automobiles, Applied Thermal Engineering 111 (2017) 1211–1231.